JOURNAL OF MATERIALS SCIENCE 33 (1998) 2673–2677

Effects of annealing treatment on the dielectric properties of manganese-modified $Pb(Fe_{2/3}W_{1/3})O_3$ ceramics

LIQIN ZHOU, P. M. VILARINHO, J. L. BAPTISTA
Departamento de Engenharia Cerâmica e do Vidro/UIMC, Universidade de Aveiro, 3800 Aveiro, Portugal

The dielectric properties of thermally treated manganese doped $Pb(Fe_{2/3}W_{1/3})O_3$ (PFW) ceramics were investigated. Modifications of the dielectric properties by thermal annealing were observed. Air annealing causes a sharpening of the dielectric permittivity and an increase of the permittivity maximum values, more pronounced as the amount of manganese dopant increases. Oxygen annealing does not cause evident variations in the dielectric permittivity curve. The presence of oxygen vacancies is evinced by thermal gravimetric measurements. The role of oxygen vacancies, as well as the associations of manganese ions with oxygen vacancies, on the annealing process, is proposed and discussed.

1. Introduction

In comparison with classic ferroelectrics, relaxors exhibit a broad and strongly frequency-dependent phase transition and the absence of macroscopic polarization at temperatures significantly below the permittivity maximum, T_0. It was suggested [1] that the lead-based ferroelectric relaxors can be viewed as having microscopic compositional fluctuations, resulting from the random distribution of different cations on the B sites of the perovskite lattice, giving a distribution of Curie points in the material and a diffuse phase transition (DPT). A superparaelectric model [2] later developed, related the relaxor behaviour to a polar cluster size effect. More recently, correlations between superparaelectric polar moments were proposed as responsible for the glass-like behaviour of relaxors [3, 4]. The diffuse nature of the phase change would be expected to depend on the ordering degree of B cations. This was first confirmed by Setter *et al.* [5], who observed that in $Pb(Sc_{1/2}Ta_{1/2})O_3$ (PST) ceramics, phase transition becomes sharper when the B site ordering is increased by thermal treatment. A long-range ordered structure, evinced by the X-ray superlattice reflections and selected-area electron diffraction pattern, was observed after thermal treatments [6, 7].

$Pb(Fe_{2/3}W_{1/3})O_3$ (PFW) has a disordered perovskite structure in which the Fe^{3+} and W^{6+} ions are randomly located on the octahedral positions. Differently from PST, the ordering of PFW ceramics is difficult to enhance by annealing treatments [8].

In the present work, modifications of the dielectric properties were achieved by thermal annealing treatments, using manganese-modified PFW ceramics. The roles of oxygen vacancies, on the ordering of the PFW perovskite structure, and of the associations of manganese ions with oxygen vacancies, on the dipolar order, are proposed and discussed.

2. Experimental procedure

The manganese incorporated into PFW ceramics was intended to substitute iron and/or tungsten on the B sites, and the compositions selected were represented by the general formula $Pb[(Fe_{2/3}W_{1/3})_{1-x}Mn_x]O_3$, in which $x = 0, 0.005, 0.01$ and 0.02.

All the samples, indicated in Table I, were prepared by the columbite precursor method, as described previously [9]. The proper ratio of Fe_2O_3 and WO_3 powders was first ball-milled in ethanol for 4 h, dried, prereacted at 1000 °C for 2 h to form the columbite type Fe_2WO_6, and then ball-milled with PbO and $Mn(NO_3)_2$. The samples were sintered at 870 °C for 2 h in air. The post-sintering thermal treatment was carried out at 800 °C for 100 h in air and oxygen, at 1 atm.

Some of the sintered and annealed samples were ground into powder and the phases were identified by X-ray diffraction analysis (XRD). The microstructure of the samples was observed in polished sections, using scanning electron microscopy (SEM). Electron diffraction studies of some samples were performed by transmission electron microscopy (TEM) using a 300 kV Hitachi H9000-NA microscope. For TEM observation, the thin foil specimens were prepared by mechanical polishing, followed by ion-beam thinning. TEM diffraction photographs were taken by using a long time exposure: 30 s.

For the dielectric measurements, sintered samples were polished and gold electrodes were sputtered on both sides. Dielectric permittivity and loss factor were measured, at different frequencies, as a function of temperature, using a Solartron 1260 impedance/Gain-Phase Analyser and a Displex APD-Cryogenics cryostat.

Thermal gravimetric measurements were carried out for some samples in order to detect possible weight losses caused by the creation of oxygen vacancies, using a Simultaneous Thermal Analysis (STA) Linseis L 81/77.

The degree of order of the PFW structure, was measured from the diffuseness coefficient, δ, which characterizes the breadth of the diffuse ferroelectric/paraelectric transition. δ was calculated by the Gaussian distribution relation [10]

$$\varepsilon_{rmax}/\varepsilon_r = \exp[(T - T_0)^2/2\delta^2] \quad (1)$$

where ε_{rmax} is the dielectric permittivity maximum, ε_r the dielectric permittivity at T, T_0 the temperature at which ε_{rmax} occurs (transition temperature).

3. Results

No change of weight occurred during thermal annealing in air, indicating that there is no lead volatilization during thermal annealing.

The XRD patterns and SEM microstructures of manganese-modified PFW ceramics were presented previously [11]. After thermal treatments, either in air or in oxygen, no visible variations in the XRD patterns and SEM microstructures were observed.

Table II shows the relative weight change after annealing in oxygen, for PFW-1Mn and PFW-2Mn. Longer annealing (>100 h) does not cause more evident weight change, indicating that 100 h annealing is sufficient to attain equilibrium.

Dielectric permittivity and loss factor of unannealed and annealed samples, as a function of temperature, at 10 kHz, are shown in Fig. 1. The common effects of the annealing treatment in air are a sharpening of the

TABLE I Studied compositions

Designation	Compositions
PFW	Pb $[(Fe_{2/3}W_{1/3})_{1-x}Mn_x]O_3$, $x = 0$
PFW–0.5Mn	Pb $[(Fe_{2/3}W_{1/3})_{1-x}Mn_x]O_3$, $x = 0.005$
PFW–1Mn	Pb $[(Fe_{2/3}W_{1/3})_{1-x}Mn_x]O_3$, $x = 0.01$
PFW–2Mn	Pb $[(Fe_{2/3}W_{1/3})_{1-x}Mn_x]O_3$, $x = 0.02$

TABLE II Relative weight change ($\Delta m/m$) after annealing at 800 °C for 100 h in oxygen at 1 atm and corresponding calculated oxygen vacancy concentration, for Pb $[(Fe_{2/3}W_{1/3})_{1-x}Mn_x]O_3$

Designation	Mn dopant concentration (cm^{-3})	$\Delta m/m$	Calculated oxygen vacancy concentration) (cm^{-3})
PFW–1Mn	1.59×10^{20}	3.2×10^{-4}	1.12×10^{20}
PFW–2Mn	3.17×10^{20}	5.9×10^{-4}	2.07×10^{20}

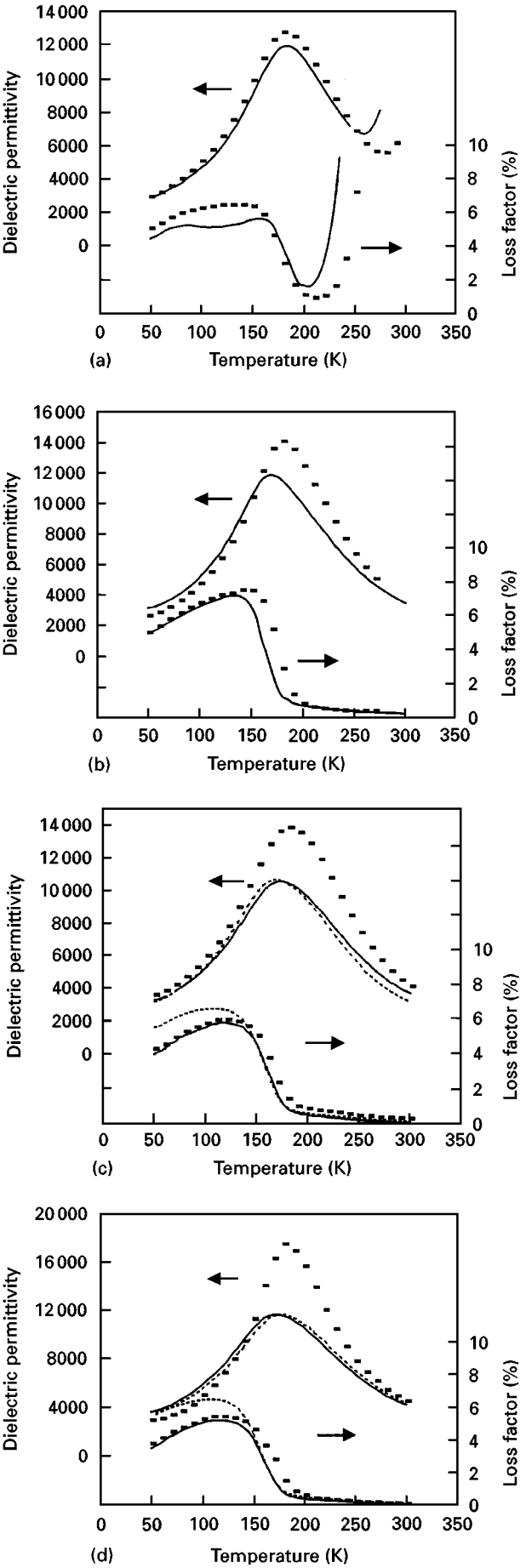

Figure 1 Dielectric permittivity and loss factor of unannealed and annealed samples, as a function of temperature, at 10 KHz, for (a) PFW, (b) PFW–0.5Mn, (c) PFW–1Mn and (d) PFW–2Mn (annealed at 800 °C for 100 h in air or oxygen). (—) Unannealed, (–) annealed in air, (- - -) annealed in oxygen.

dielectric permittivity and an increase of the permittivity maximum value. The annealing effect is enhanced with increasing amount of manganese dopant.

For the oxygen annealing, from Fig. 1c and d, we can see that there is almost no observable difference in the dielectric permittivity curve between unannealed and oxygen-annealed PFW–1Mn and PFW–2Mn samples, except for a very small shift of the transition temperature. However, in the loss factor curve, the loss in the ferroelectric region is significantly higher for the oxygen-annealed samples, being almost the same in the paraelectric region.

The dielectric properties, including dielectric permittivity maximum, ε_{rmax}, transition temperature, T_0, and the diffuseness coefficient, δ, at 10 and 100 kHz, for the unannealed and annealed samples, are shown in Table III, from which the variations of dielectric properties after annealing become clearer. The sharpening of the dielectric permittivity corresponds to the decrease of the diffuseness coefficient, δ.

Fig. 2 gives the manganese content dependence of the air-annealing variations in the permittivity maximum value, $\Delta\varepsilon_{rmax}/\varepsilon_{rmax}$ ($\Delta\varepsilon_{rmax} = \varepsilon_{rmax(a)} - \varepsilon_{rmax}$, ε_{rmax} and $\varepsilon_{rmax(a)}$ being the permittivity maximum for the same sample before and after annealing) and the air-annealing variations in the diffuseness coefficient, $\Delta\delta/\delta$ ($\Delta\delta = \delta - \delta_{(a)}$, δ and $\delta_{(a)}$ defined as ε_{rmax} and $\varepsilon_{rmax(a)}$). As can be seen, $\Delta\varepsilon_{rmax}/\varepsilon_{rmax}$ and $\Delta\delta/\delta$ increase almost linearly with the increase in manganese content.

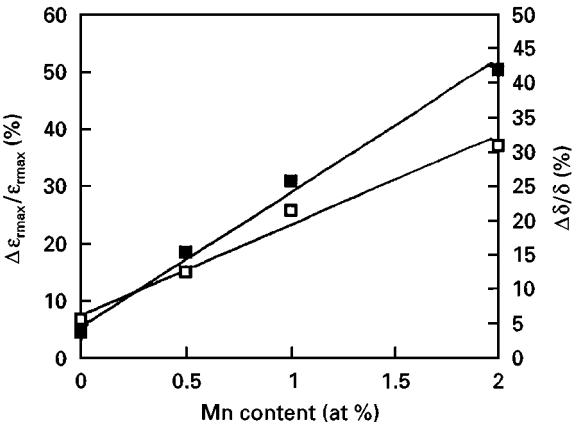

Figure 2 Annealing variations in the (■) dielectric permittivity maximum $\Delta\varepsilon_{rmax}/\varepsilon_{rmax}$ and in the (□) diffuseness coefficient $\Delta\delta/\delta$, as a function of manganese content (annealed at 800 °C for 100 h in air).

4. Discussion

For manganese-doped samples, the manganese ion located at B sites will carry an excess negative charge which, in order to maintain the charge balance, was suggested to be dominantly compensated by oxygen vacancies [11]. During annealing in oxygen, the oxygen from the atmosphere could fill the oxygen vacancies accompanied by the corresponding valence change of one of the cations, most probably Mn^{2+} to Mn^{3+} or even Mn^{4+}. To confirm the existence of oxygen vacancies in manganese-doped PFW ceramics, gravimetric measurements were carried out, with the relative weight change indicated in Table II. The calculated oxygen vacancy concentration according to the relative weight change, $\Delta m/m$, is also shown in Table II, being not far from and with the same trend as the dopant concentration values, 1.59×10^{20} for 1 at% Mn and 3.17×10^{20} for 2 at% Mn. This result indicates that for sintered manganese-doped PFW samples, the manganese ions located at B sites are predominantly compensated by oxygen vancancies, which could be filled by annealing in oxygen with a concomitant change in the manganese oxidation state. This implies that an increase in O_2 vapour pressure from its value during sintering in air, to 1 atm O_2 during annealing at 800 °C, can alter the vacancy equilibrium concentration in a significant way. A smaller value of the calculated oxygen vacancy concentration than that of the dopant concentration probably points to an equilibrium between Mn^{3+} and Mn^{4+} in oxygen-annealed samples. For other compositions such as PFW and PFW–0.5Mn, the weight change would be too small to be measured reliably under our conditions, and therefore the measurement was not attempted.

After oxygen annealing, the loss in the ferroelectric region increases while that in the paraelectric region does not change, as shown in Fig. 1c and d. It has been suggested that in ferroelectric materials, lattice defects inhibit the domain-wall movement, consequently decreasing the losses in the ferroelectric region [12]. The lower loss in the ferroelectric region for unannealed samples is probably due to the presence of the oxygen vacancies. Owing to the filling of these vacancies after oxygen annealing, the loss in the ferroelectric region increases.

TABLE III Dielectric properties of unannealed and annealed $Pb[(Fe_{2/3}W_{1/3})_{1-x}Mn_x]O_3$ ceramics, at 10 and 100 kHz (annealed at 800 °C for 100 h in air or oxygen at 1 atm)

Designation	Thermal treatment	Frequency (KHz)	ε_{rmax}	T_0(K)	δ(K)
PFW	Unannealed	10	12 180	184	53
		100	11 550	186	54
	Annealed in air	10	12 730	181	50
		100	12 240	183	51
PFW–0.5Mn	Unannealed	10	11 910	172	56
		100	11 440	177	57
	Annealed in air	10	14 110	180	49
		100	13 480	184	50
PFW–1Mn	Unannealed	10	10 660	170	56
		100	10 450	175	57
	Annealed in air	10	13 960	180	44
		100	13 740	182	45
	Annealed in oxygen	10	10 760	166	56
		100	10 520	171	57
PFW–2Mn	Unannealed	10	11 660	168	55
		100	11 500	173	56
	Annealed in air	10	17 510	180	38
		100	17 400	181	38
	Annealed in oxygen	10	11 670	172	55
		100	11 510	177	56

Different variations in the dielectric properties for air and oxygen annealing treatments were observed, as shown in Fig. 1 and Table III. Air annealing significantly causes the decrease of diffuseness and the degree of decrease increases with the increase in manganese content. Almost no difference was observed in the dielectric permittivity curve between the samples before and after oxygen annealing.

Contrary to PST, the ordering of PFW ceramics cannot be easily enhanced by annealing treatment [8]. However, the sharpening of the dielectric permittivity peak after air annealing points to a modification of the polarization behaviour. Variations in the permittivity maximum value seem not to be a good indication to interpret such modification because increases in permittivity after thermal annealing treatments were observed for PST single crystals [5] and the opposite effect was observed for PST ceramics [13]. However, it has been commonly recognized that an increase in lattice order leads to a decrease in diffuseness, i.e. the sharpening of the dielectric permittivity [2, 5, 13, 14], as was also observed here. Taking the decrease of diffuseness as an indication of an increase in lattice order, the annealing study reported here seems to indicate that the oxygen vacancies, present in manganese-doped PFW ceramics, could significantly increase the possibility of rearranging Fe^{3+} and W^{6+} on B sites. This is structurally reasonable, because the ordering of the perovskite structure by annealing is a rearrangement process of Fe^{3+} and W^{6+} and the presence of vacancies can favour the diffusion of B cations.

The lattice order can be evinced by superlattice reflections in XRD and TEM diffraction. Although no superlattice reflections related to B cation order were observed in XRD for all the samples, as shown in Fig. 3, for air-annealed PFW–2Mn, weak F spots corresponding to 1 : 1 B cation order were observed by TEM, whereas those superlattice spots were almost invisible in unannealed PFW–2Mn, as shown in Fig. 4. This indicates that B cation order is indeed increased after air annealing, as discussed above.

An increase in dipole order has been considered to be responsible for the sharpening of the dielectric permittivity curves of PMN and $Pb(Zn_{1/3}Nb_{2/3})O_3$ (PZN) when forming solid solutions with $PbTiO_3$ (PT) [15]. A similar effect could also take place in manganese-doped PFW where the manganese ions are predominantly compensated by oxygen vacancies as discussed above. The dipoles formed by association of the manganese ions with oxygen vacancies may couple to the spontaneous dipoles present in PFW, enhancing long-range dipolar interactions and then promoting dipolar order. If thermal annealing helps to align the associations of defects, the increase in dielectric permittivity maximum could be due to this contribution.

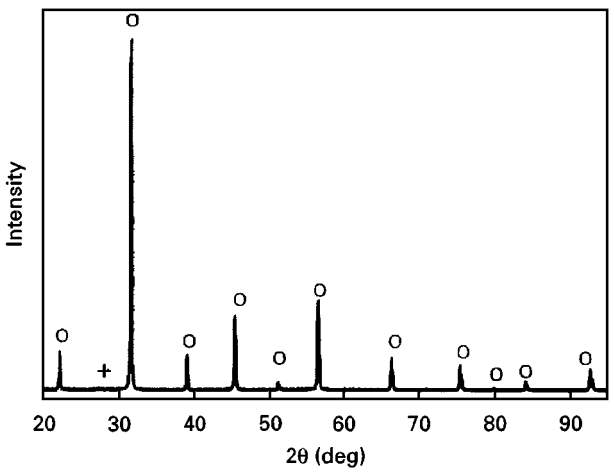

Figure 3 XRD pattern of air-annealed PFW–2Mn ceramics. (○) PFW, (+) $PbWO_4$.

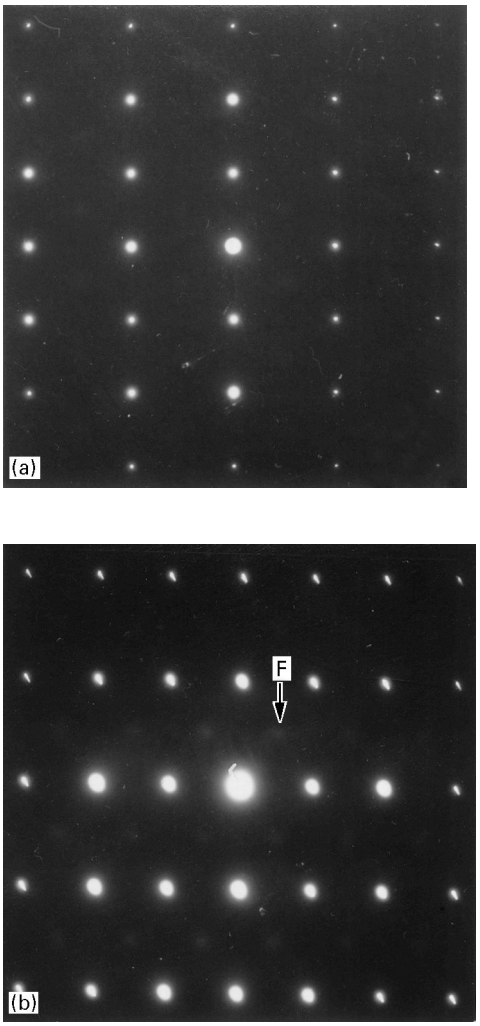

Figure 4 ⟨1 1 0⟩ zone-axis diffraction pattern of PFW–2Mn (a) before and (b) after air annealing. The superlattice F spots are indicated in (b).

5. Conclusion

Air annealing causes the sharpening of the dielectric permittivity and the increase of the permittivity maximum value, for manganese-doped PFW ceramics. These effects increase with the increase in the manganese concentration. Oxygen annealing does not cause evident variations in the dielectric permittivity curve, but the loss in the ferroelectric region increases. The presence of oxygen vacancies is evinced by thermal gravimetric measurements. The reasons for the

thermal annealing observations are discussed. It is suggested that the oxygen vacancies present in manganese-doped PFW promote the rearrangement of Fe^{3+} and W^{6+} on B sites and increase lattice order. Experimental evidence for the increase in lattice order was obtained by TEM observations. It is further suggested that associations of manganese ions with oxygen vacancies could couple to the spontaneous dipoles, enhancing long-range dipolar interactions and then promoting dipolar order which could account for the enhancement of the value of the dielectric maximum.

Acknowledgement

The financial support from the Orient Foundation is greatly acknowledged.

References

1. G. A. SMOLENSKII, V. A. ISUPOV, A. I. AGRANOVSKAYA and S. N. POPOV, *Sov. Phys. Solid State* **2** (1961) 2584.
2. L. E. CROSS, *Ferroelectrics* **76** (1987) 241.
3. D. VIEHLAND, J. F. LI, S. J. JANG and L. E. CROSS, *Phys. Rev. B* **43** (1991) 8316.
4. D. VIEHLAND, S. J. JANG and L. E. CROSS, *J. Appl. Phys.* **68** (1990) 2916.
5. N. SETTER and L. E. CROSS, *ibid.* **51** (1980) 4356.
6. N. SETTER and L. E. CROSS, *J. Mater. Sci.* **15** (1980) 2478.
7. M. P. HARMER, A. BHALLA, B. FOX and L. E. CROSS, *Mater. Lett.* **2** (4A) (1984) 278.
8. P. M. VILARINHO, PhD thesis, Aveiro University, Portugal (1994).
9. LIQIN ZHOU, P. M. VILARINHO and J. L. BAPTISTA, *Mater. Res. Bull.* **29** (1994) 1193.
10. S. R. PILGRIM, A. E. SUTHERLAND and S. R. WINZER, *J. Amer. Ceram. Soc.* **73** (1990) 3122.
11. LIQIN ZHOU, P. M. VILARINHO and J. L. BAPTISTA, *Mater. Res. Bull.* **31** (1996) 699.
12. P. V. LAMBECK and G. H. JONKER, *Ferroelectrics* **22** (1978) 729.
13. F. CHUN, M. DAGLISH and N. SETTER, in "Proceedings of the Third Euro-Ceramics", Madrid Spain, edited by P. Durán and J. F. Fernández, Faenza Editrice Iberica S.L., Vol. 2 (1993) p. 91.
14. J. CHEN, H. M. CHAN and M. P. HARMER, *J. Amer. Ceram. Soc.* **72** (1989) 593.
15. C. A. RANDALL, A. S. BHALLA, T. R. SHROUT and L. E. CROSS, *J. Mater. Res.* **5** (1990) 829.

Received 26 November 1996
and accepted 13 February 1998